

# MAGNETIC PROPERTIES OF LASER-TREATED FINEMET

Peter KOLLÁR

Institute of Physics, Faculty of Sciences, P. J. Šafárik University, Park Angelinum 9, 041 54 Kočice, tel +421-55-6221128, e-mail: [kollar@kosice.upjs.sk](mailto:kollar@kosice.upjs.sk)

## SUMMARY

The positive influence of the laser treating on the decrease of power losses of many soft magnetic materials (as well as nanocrystalline FINEMET) is well known. The surface defects can cause refinement of the domain structure producing small domains with movable domain walls. Such a refinement is one of the ways how to reduce dynamic loss at higher frequencies which is dominant in the total power loss. What is the role of surface defects caused by the excimer laser treatment on the bulk and surface-layer coercivity, domain structure and anisotropy, that is the question which we would like to answer in this article.

**Keywords:** FINEMET, nanocrystalline material, excimer laser, domain structure, coercivity, anisotropy

## 1. INTRODUCTION

FINEMET ( $\text{Fe}_{73.5}\text{Cu}_1\text{Nb}_3\text{Si}_{13.5}\text{B}_9$ ) is a nanocrystalline material with excellent soft magnetic properties [1]. Though the losses are very low compared to other crystalline metallic soft magnets, the fraction of the frequency dependent dynamic losses in FINEMET is high [2] and this fact offers a large potential for further improvement.

Experimental results [3-5] show that laser treatment is one of way how to reduce the power losses of soft magnetic materials, especially of FINEMET.

## 2. EXPERIMENTAL

The amorphous  $\text{Fe}_{73.5}\text{Cu}_1\text{Nb}_3\text{Si}_{13.5}\text{B}_9$  ribbons (14.9 mm wide and  $21\mu\text{m}$  thick) used for surface modification experiments were supplied by Vacuumschmelze (Hanau). For magnetic measurements and domain observations we cut 110 mm long and approximately 2.77 mm wide samples out of these ribbons. Since the nanocrystallization leads to the embrittlement of material, the laser treatment was performed prior to the heat treatment on the non-wheel side of the samples. A set of parallel grooves ( $60\mu\text{m}$  wide and a  $12\mu\text{m}$  deep) or pitted lines (each pit is  $12\mu\text{m}$  deep) perpendicular to the sample's longitudinal direction and with various spacing was produced on the non-wheel side of the ribbon surface, by multiple overlapping pulses of XeCl-excimer laser radiation.

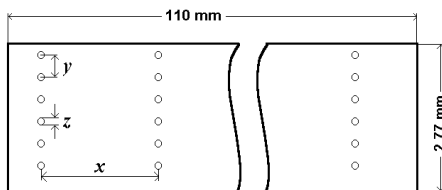
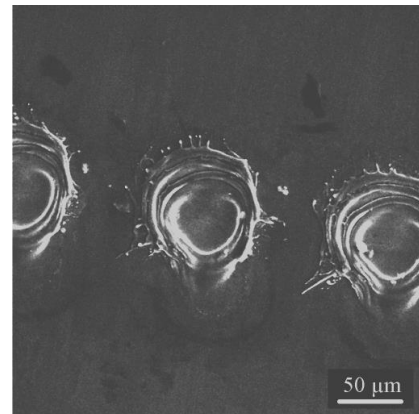
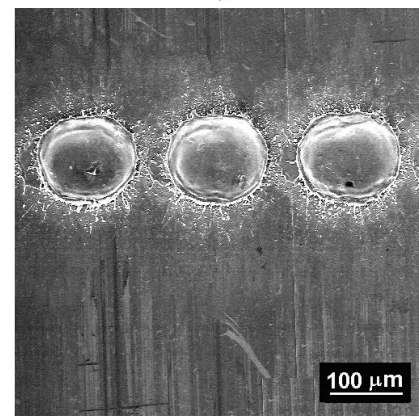


Fig. 1. Arrangement of pitted lines. x-spacing of pitted lines, y-the distance between two pits, z-diameter of the pit.

The arrangement of pitted lines is shown in Fig. 1, and micrographs of circular pits (observed by SEM) of two examples of various arrangement are shown in Fig. 2.



a)



b)

Fig. 2. SEM micrographs of circular pits on the sample a) with small pit's density ( $x=10\text{ mm}$ ,  $y=150\mu\text{m}$ ), b) with high pit's density ( $x=2\text{ mm}$ ,  $y=50\mu\text{m}$ ).

The surface treated samples were annealed in evacuated quartz tubes at 580 °C for one hour and then quenched in a water bath at room temperature. Saturated hysteresis loops (in a maximum field of 16 kA/m) of about 50 nm thick surface layers were measured on the non-wheel side of ribbons by a dc hysteresisgraph based on the transversal Kerr effect and the coercivity was calculated from these loops [6]. The measured area was  $2.77 \times 1 \text{ mm}^2$  (width of sample  $\times 1 \text{ mm}$  along the ribbon axis). To detect the influence of laser treatment on the bulk magnetic properties we have used a dc fluxmeter based hysteresisgraph enabling to measure hysteresis loops in magnetic fields up to 20 kA/m. From these loops we calculated bulk coercivity. The power losses were measured in a frequency range from 3.2 Hz to 20 kHz at different polarisations using a computer controlled digital hysteresis recorder [4]. Large domains on the non-wheel side were visualised by a computer-controlled set-up based on the Kerr effect [7]. Small domains near circular pits were investigated by means of a JEOL JSM 840 scanning electron microscope using backscattered electron imaging mode [8].

### 3. POWER LOSSES

D. Ramin et al. [4] have found that power losses of laser-treated in comparison with untreated FINEMET at a maximum polarisation of 0.9 T versus frequency, fig.3. The circular pits of treated sample had a distance of 150  $\mu\text{m}$  on a line with a line spacing of 10 mm. It can be seen that the losses at low frequencies are increased due to the surface laser treatment whereas at higher frequencies the losses of the untreated sample are lower than those of the laser-treated ones. This is caused by the decrease of dynamic losses by surface treatment, which become dominant at frequencies above 600 Hz. [4]

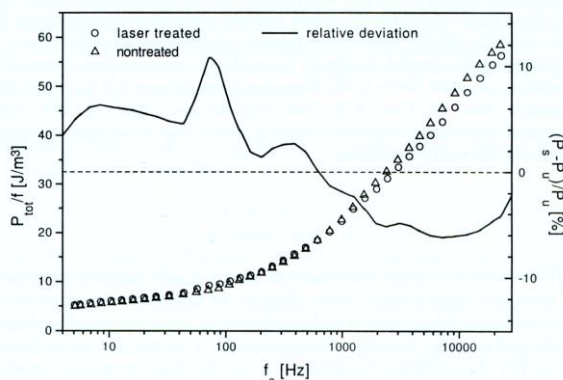


Fig.3. Total power losses of surface treated (s) and untreated (u) samples and their relative deviation vs. frequency [4].

It was found that decrease of the losses by laser surface treatment can not be archived if the depth of the defect is smaller than half of the ribbon's thickness regardless if grooves or discrete pits are used [4].

### 4. BULK AND SURFACE-LAYER COERCIVITY

Because the grooves produced by excimer laser are only a few  $\mu\text{m}$  deep, no significant influence of the laser treatment on the bulk coercivity was observed. The depth of the grooves is larger than the thickness of the surface layer participating in the reflection of the light used to measure the surface layer hysteresis loop, and that is why we can expect that laser treatment can influence the surface-layer coercivity significantly. Fig. 4 shows the dependence of the surface-layer coercivity measured on the non-wheel side along the ribbon axis in 1 mm steps. We can see that the coercivity increases steeply in the area of the laser produced lines, reaching the values approximately four times larger than in the area between these laser lines [9].

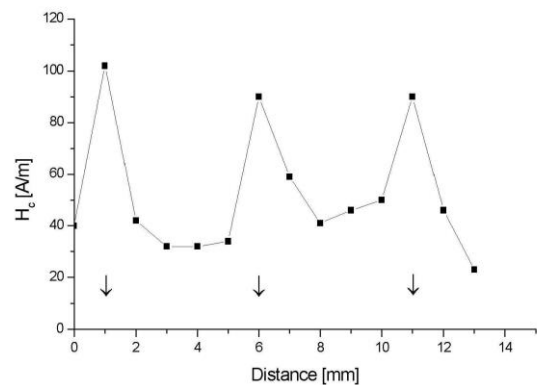


Fig. 4. The dependence of the surface-layer coercivity measured on the non-wheel side along the ribbon axis of FINEMET with perpendicular scratched lines produced by excimer laser with 5 mm spacing. Arrows show the positions of scratched lines [9].

The dependence of the bulk coercivity on the reciprocal value of the spacing of pitted lines is shown in Fig. 5. The rise of the coercivity with the increase of the density of the pitted lines is attributed to the increase in the number of pits, which play the role of pinning centres [10].

The surface-layer coercivity near the scratched grooves produced by laser treatment is larger than in the area between them (Fig. 4). Therefore we expected to find the same periodical variations (due to the presence of pitted lines) in the surface-layer coercivity scanned along the ribbon.

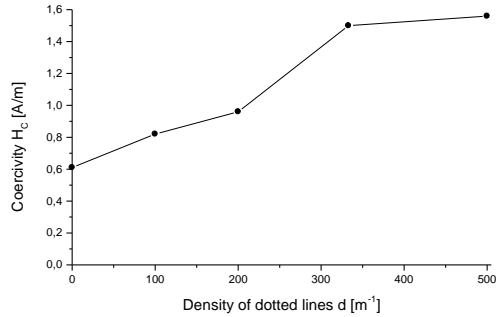


Fig. 5. The dependence of the bulk coercivity on the reciprocal value of the spacing of pitted lines.

However, no such variations were found. This would mean that the domain structure of ribbons with pits is probably very different from that observed on ribbons with grooves and our aim was to prove this assumption [10].

## 5. DOMAIN STRUCTURE

The domain structure on the surface treated FINEMET ribbon (Fig. 6) differs from the domain structure of the non-treated sample [11], which consists of wide (few 100  $\mu m$ ) domains, separated by  $180^\circ$  domain walls.

The excimer laser treatment removes material of the ribbon surface without any other influence (as for example a mechanical stress or crystallization) on the sample. The grooves perpendicular to the ribbon axes prepared by laser treatment produce local demagnetizing field in the surface layer and they also change the domain structure in the area near to the lines. In the middle part between two scratched lines wide domains with the magnetic polarization vector oblique to the ribbon axis are present. As a consequence of demagnetization field, narrow domains with in-plane lying magnetic polarization vector perpendicular to the ribbon axis are present near the scratched lines. The domain structure shows that no additional stresses are caused by the excimer laser treatment. The magnetization process is realized in the middle part between two scratched lines by the movement of domain walls, that is why the surface coercivity is lower than in the area of scratched lines where the magnetization process is realized by the rotation of the magnetic polarization vector. The influence of perpendicular domains (with non-moving walls) on the bulk magnetization process is negligible, because no difference between the bulk dc coercivity of treated and non-treated samples was detected. [9]

Wide domains are also visible in domain patterns of FINEMET with pitted lines (with 10 mm spacing, consisting of pits with diameter of 50  $\mu m$  with a separation of 150  $\mu m$ ), perpendicular to the ribbon axes visible in the bottom third of the sample in Fig.

7., observed both with longitudinal and transverse magneto-optical sensitivity. This is because the magnetization vector in these domains is oriented oblique to the ribbon axis and its orientation changes continuously between two pitted lines.

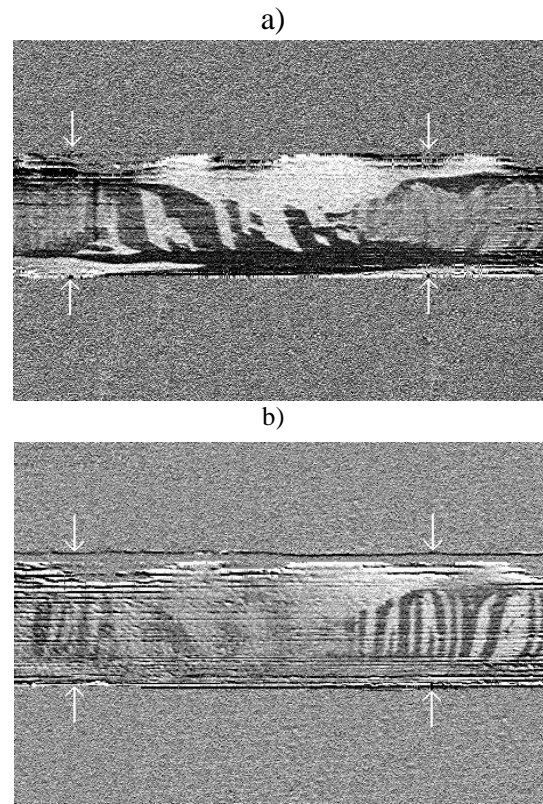


Fig. 6. The domain structure on the non-wheel side of FINEMET ribbon with perpendicularly scratched lines. The perpendicular narrow domains are near to the scratched lines and oblique domains are in the middle part between two scratched lines. Sensitivity axes are along the ribbon axis a) and perpendicular to the ribbon axis b). Arrows show the positions of scratched lines.

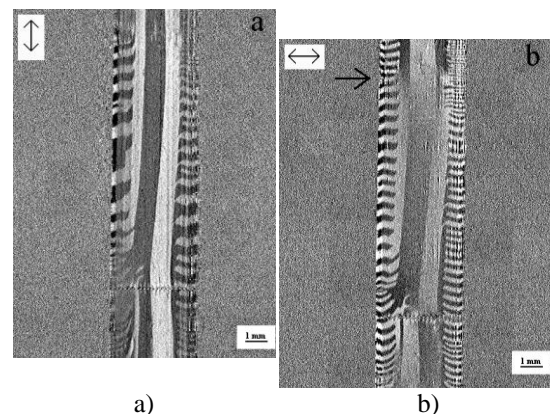


Fig. 7. The domain structure of the laser-treated FINEMET ribbon in the demagnetizing state influenced by pitted line, observed by means of the Kerr technique. Arrows indicate the magneto-optical sensitivity axes ( $\leftrightarrow$ ).

This change in orientation is seen as a change in contrast. Approximately in the middle between two lines the orientation of the magnetization vector is exactly parallel to the ribbon axis. In this area the contrast between two domains, observed with transverse sensitivity, disappears (see  $\rightarrow$  in Fig. 7b). It is evident from Fig. 7a, taken with longitudinal sensitivity, that the presence of pitted lines does not significantly influence the size of longitudinal component of the magnetization vector in wide domains. On the other hand, it is seen in Fig. 7b, taken with transverse sensitivity, that the transverse component of the magnetization vector changes discontinuously its orientation at the pitted line. We can suppose that the pitted line divides wide domains into two parts (at least in the surface layer). Small domains (few  $10 \mu\text{m}$  wide), with  $180^\circ$  domain walls are formed near to laser ablated circular pits and they are the product of domain refinement (branching) [11]. These domains are visible only in picture taken with longitudinal sensitivity (Fig. 7a) and that is why we suppose that the magnetization vector in these domains is oriented antiparallel to the surrounding wide domains. For the detailed observation of small domains it is more suitable to investigate them by SEM, which can visualize also domain walls, Fig. 8.

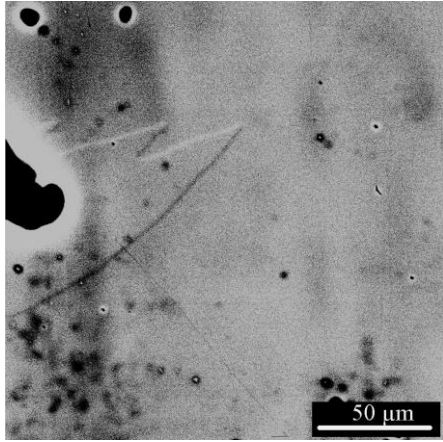


Fig. 8. The small domain produced by domain branching near to the circular pit, observed by SEM.

The absence of domains typical for areas with induced stresses (zig-zag domains) in close proximity to circular pits allows us to state that the circular pits produced by laser treatment do not introduce mechanical stresses which would influence the domain structure.

At the edge of the nanocrystalline ribbon transverse narrow domains are present. Similar domains formed due to the mechanical stresses at the edge of the ribbon were investigated in as-quenched FINEMET [12].

Formation of small domains on opposite sides of the pit along the longitudinal axis of the ribbon as a product of domain branching is possible if the total

energy of the small domains is smaller than the reduction of the energy of the magnetic field in the pit. The size of such a small domain (a model is in Fig. 9) is determined by the total energy minimum.

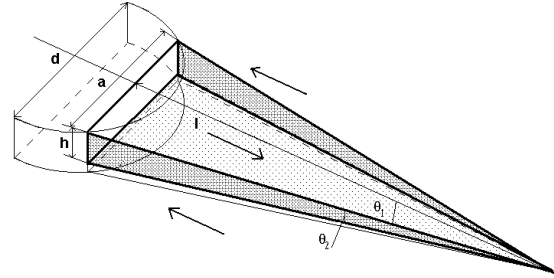


Fig. 9. The model of the small domain in close proximity to circular pit ( $d$  is the diameter of the pit, parameters of the domain are length  $l$ , height  $h$  and maximum width  $a$ ).

From the condition for minimizing the total energy we have calculated the length and the total energy of the small domain [13]:

$$l_0 = 3 \sqrt[3]{\frac{I_s^2 \delta_w (4h^3 a + a^3 h)}{8\mu_0 \gamma_w \left(h + \frac{a}{2}\right)}} \quad (1)$$

$$E_{tot0} = \frac{3}{4} \sqrt[3]{\frac{I_s^2 \delta_w (4h^3 a + a^3 h) \left[\gamma_w \left(h + \frac{a}{2}\right)\right]^2}{\mu_0}} \quad (2)$$

In Eqs. (1, 2) we used the expression for the energy of the domain wall per unit area:

$$\gamma_w = 2\sqrt{A_{ex} \langle K \rangle}$$

where  $\langle K \rangle$  denotes the effective anisotropy constant calculated according the random anisotropy model given by  $\langle K \rangle = K_1^4 d^6 / A_{ex}^3$  [14]. The anisotropy constant of FeSi grains of FINEMET is  $K_1 = 8000 \text{ J/m}^3$ , the exchange constant  $A_{ex} = 10^{-11} \text{ J/m}$ , the grain diameter  $d = 10 \text{ nm}$ , the thickness of the domain wall  $\delta_w = 2,7 \mu\text{m}$  [15] and putting all required constants in Eqs. (1) and (2) we have obtained the length  $l_0 = 763 \mu\text{m}$  and total energy of the domain  $E_{tot0} = 7.96 \times 10^{-8} \text{ J}$ . The calculated length of the domain is in a good agreement with the observed one [13].

## 6. INDUCED ANISOTROPY

The domain patterns of laser-non-treated FINEMET consist of wide, slightly wavy domains, parallel to the longitudinal ribbon axis that are separated by  $180^\circ$  domain walls [16], while the domain structure of samples is significantly influenced by laser treatment (circular pits with  $150\ \mu\text{m}$  diameter, with separation of  $200\ \mu\text{m}$ ), Fig.10.

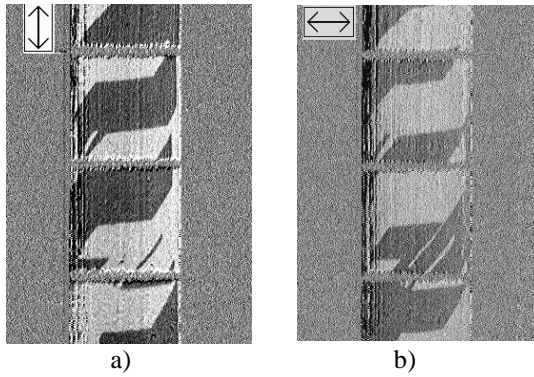


Fig. 10. The domain structure of the laser-treated FINEMET ribbon in the remanent state, observed by means of the Kerr technique, width of domains  $a=1.5\ \text{mm}$ . The magnetooptical sensitivity axes are indicated by arrows ( $\leftrightarrow$ ).

The domains with the in-plane magnetic polarization vector with dominant component perpendicular to the ribbon axis are created as a consequence of the strong demagnetizing field produced by circular pits. We assume that this demagnetizing field produces anisotropy, with the easy axis perpendicular to the ribbon axis, which is stronger than the form anisotropy of the relatively long, narrow ribbon. As a consequence of the both mentioned anisotropies, the wide transverse stripe domains, with  $180^\circ$  domain walls, are formed in the middle part of the ribbon. The closure domains were created at the edge of the ribbon to decrease the magnetostatic energy [17]. The influence of the laser formed pits on the creation of these wide domains is evident not only in the close proximity of the pits but almost along the sample.

The shape and tilting of the hysteresis loops of the treated is compared with the shape and tilting of the hysteresis loop of the nontreated sample, Fig. 11.a). The shape of the hysteresis loop of the laser-treated sample is “wavy”, because the magnetization process is realized simultaneously by domain wall displacement of the domain with large perpendicular component of spontaneous magnetic polarization vector and rotation of spontaneous polarization vector within magnetic field range in which for FINEMET is typical only rotation of spontaneous magnetization polarization vector. The hysteresis loop of non treated samples is steeper, because its domain structures consist of larger

number of movable domain walls, but on the other hand they are wider, it means, the coercivity rises with the density of circular pits, which act as the domain wall pinning centres.

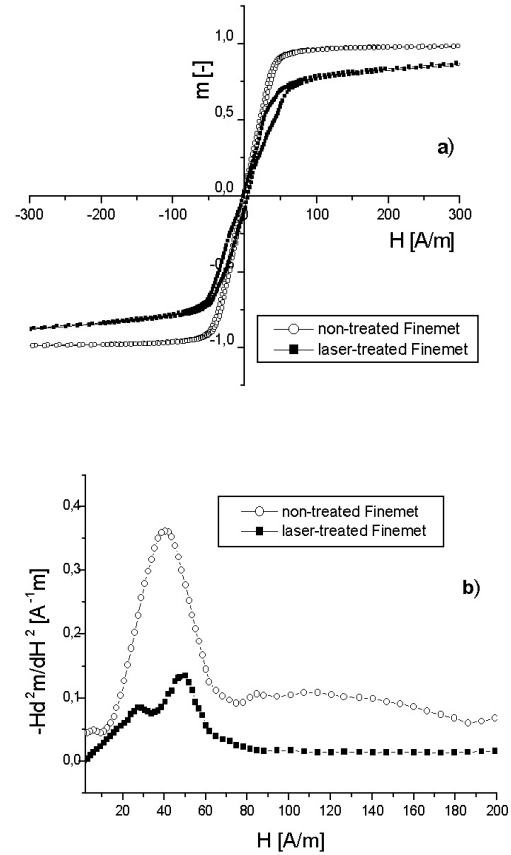


Fig 11. a) The hysteresis loops of the non-treated and laser-treated FINEMET. b) Corresponding magnetic anisotropy distributions of the non-treated and laser-treated FINEMET.

Based on the Stoner-Wohlfarth model, the distribution of magnetic anisotropy can be obtained from the second derivative of the magnetization curve [18, 19], provided that the easy axes are oriented at right angles to the applied magnetic field. From the second derivative of the magnetization curve of both non-treated and laser-treated samples we have obtained the magnetic anisotropy distribution.

$$P(H) = -H \frac{d^2 m}{dH^2}, \quad (3)$$

where  $m = \frac{M}{M_S}$  is the macroscopic reduced magnetization of the sample and  $H$  is the applied field.

Fig.11.b) shows anisotropy distribution corresponding to the demagnetization curve (a part of hysteresis loop between remanence and

saturation) of both samples. The shape of the magnetic anisotropy distribution  $P(H)$  for laser-treated sample consist of two peaks. The additional peak (in comparison with the non-treated sample) occurs at lower magnetic field of  $H^K = 29 A/m$ .

Using equation  $2K = \mu_0 M_S H^K$  we have calculated the value of the constant of the induced transverse magnetic anisotropy to be  $K_U = 18 J/m^3$ . This means that the anisotropy induced by laser treatment is comparable to the anisotropy induced by annealing in transverse magnetic field, which has the value of  $15 J/m^3$ , the magnetic anisotropy is  $24 J/m^3$  [20].

The calculated laser-induced anisotropy constant can be used for the calculation of domain width, expressed by the equation [17]

$$a = \frac{\pi^3 b \sqrt{A_{ex}}}{2T \sqrt{K_u}}, \quad (4)$$

$b$  is the width of the ribbon,  $T$  is the thickness of the ribbon,  $A_{ex}$  is the exchange constant and  $K_U$  is the constant of magnetic anisotropy. The calculated width of the domains (for  $b = 2.77 mm$ ,  $T = 21 \mu m$ ,  $A_{ex} = 10^{-11} J/m$ ),  $K_U = 19 J/m^3$  is about  $1.52 mm$ , which is in a good agreement with the width of domains observed in the remanent state (Fig. 10).

## 7. CONCLUSION

Investigating the influence of laser treatment on magnetic properties of FINEMET we obtained that:

- The grooves and the pits arranged into the line perpendicular to the ribbon axis produced by excimer laser act as sources of demagnetizing field without any other harmful influence on the domain structure.
- The circular pits represent pinning centres for domain wall motions.
- In the close proximity to the circular pits the demagnetizing field causes domain branching producing one small domain with reverse oriented magnetization vector. This domain branching is responsible for the reduction of losses at higher frequencies
- Demagnetizing field created by the pits produces anisotropy perpendicular to the ribbon causes perpendicular anisotropy which is comparable to the anisotropy induced in Finemet by annealing in transverse magnetic field.

## REFERENCES

[1] Yoshizawa Y., Oguma S. and Yamauchi K.: J.

- Appl. Phys. 64 (1988) 6044
- [2] Wittwer C., Riehemann W., and Heye W.: J. Magn. Magn. Mater. 133 (1997)
- [3] Ramin D., Weidenfeller B. and Riehemann W.: Mat. Sci. Eng., A226-228 (1997) 590.
- [4] Ramin D., Riehemann W.: Acta Physica Slovaca, vol. 48, 6, 1998 679
- [5] Weidenfeller B., Riehemann W.: J. Magn. Magn. Mater., 133 (1997) 177-179.
- [6] Kollár P., Skyba P., Potocký L., Juránek Z.: Elektrotechn. Čas. 38 (1987) 283-286
- [7] Kuzmiński M., Fink-Finowicki J. and Siemko A.: Acta magnetica, Suppl. 90, (1990) 147.
- [8] Pogány L., Vértesy Z., Sándor S., Konczos G.: Proc XI th. Int. Cong. on Electron Microscope, 1737, Kyoto 1986.
- [9] Kollár P., Ramin D., Zeleňáková A., Riehemann W., Kužminskim.: JMMM 302 (1999) 301-304
- [10] Zeleňáková A., Vértesy Z., Kollár P., Kuzmiński M., Ramin D., Riehemann W.: Scripta Materialia 44 (2001) 616-617
- [11] Schäffer R., Hubert A., Herzer G.: J. Appl. Phys. 69 (8) 1991, 5325-5327
- [12] Vértesy Z., Kisdi-Koszó E., Kuzmiński M., Lachwicz H. K.: Phys. stat. sol. (a) 143, 1994, 149.
- [13] Zeleňáková A., Kollár P., Vértesy Z., Kuzmiński M., Ramin D., Riehemann W.: Acta Physica Slovaca 50 (2000) 501-506
- [14] Herzer G.: Scripta Metallurgica and Materialia, Vol. 33 (1995) 1741-1756
- [15] Reininger T., Hofmann B., Kronmüller H.: J. Magn. Magn. Mater., 111 (1992) L220-L224.
- [16] Hubert A., Schäffer R.: Magnetic domains, Springer-Verlag Berlin Heidelberg 1998, Section 3.7.5.
- [17] Reininger T., Kronmüller H.: phys. stat. sol. (a) 129 (1992) 247-254.
- [18] Franco V., Conde A.: Applied Physics Letters, Vol. 74, 25, (1999) 3875-3877.
- [19] Franco V., Conde C. F., Conde A.: J. Magn. Magn. Mater., 185 (1998) 353-359.
- [20] Yoshizawa Y., Yamauchi K.: IEEE Trans. on Mag., 25 (5) 1989, 3324-3326.

## BIOGRAPHY

Peter Kollár was born on April 23, 1960. He graduated (MSc.) with distinction from the Faculty of Science at the P.J. Šafárik University in Košice in 1983. He defended his PhD. (CSc.) thesis Surface magnetic properties of FeB based amorphous alloys in 1990. Since 1996 he is associated professor and since 2001 he is the head of the Department of Solid State Physics of the Institute of Physics, Faculty of Sciences, P. J. Šafárik University. His scientific research is focused on the investigations of magnetic properties of soft magnetic materials.